1994ApJ...425..127G

THE ASTROPHYSICAL JOURNAL, 425:127–131, 1994 April 10
© 1994. The American Astronomical Society. All rights reserved. Printed in U.S.A.

HIGH-RESOLUTION MEASUREMENTS OF NH_3 ABSORPTION TOWARD CASSIOPEIA A

R. A. GAUME,[1] T. L. WILSON,[2] AND K. J. JOHNSTON[1]
Received 1993 August 13; accepted 1993 October 14

ABSTRACT

We have observed NH_3 absorption against the bright supernova remnant Cassiopeia A. The 3″ resolution VLA map shows absorption against the brightest continuum peak in the NH_3 $(J, K) = (1,1)$ inversion transition. The absorption maximum is at R.A. = $23^h20^m54^s.8$, Decl. = +50°32′23″ (1950.0), projected against the region of brightest continuum emission. This is near where the deepest absorption was found with the 40″ beam of the Effelsberg 100 m telescope. The apparent optical depth of the NH_3 absorption, when averaged over the strongest continuum emission, is ≈ 0.1. The NH_3 absorption region has a size of at least 60″.

In order to characterize the NH_3-containing cloud, $J = 1$–0 and $J = 2$–1 spectra of CO and ^{13}CO were taken for the nearest CO cloud, 20″ from the NH_3 maximum. In addition, a spectrum of the $J = 2$–1 transition of ^{13}CO was taken at the position of maximum NH_3 absorption. These CO and ^{13}CO data show that the V_{lsr} of the cloud is -39 km s^{-1}, the FWHP line width is 3.5 km s^{-1}, and the column density, $N(H_2)$, is 3×10^{21} cm^{-2}. The density, $n(H_2)$, is about 1000 cm^{-3} and kinetic temperature, T_k, is 18 K. The virial mass estimated for this cloud is about 60 times the mass obtained from CO data.

It is likely that the NH_3 absorption and CO emission arise in the same physical region. This region is significantly warmer than a typical dark dust cloud, shows a significantly larger line width, and has about 0.1 of the cloud mass in H I. The $n(H_2)$ and $N(H_2)$ values are comparable to dark dust cloud values. The enhanced kinetic temperature may be caused by an increased cosmic-ray rate, or by cloud-cloud collisions.

Subject headings: ISM: individual (Cas A) — ISM: molecules — radio lines: ISM — supernova remnants

1. INTRODUCTION

The supernova remnant (SNR) Cassiopeia A is an intense continuum source with a diameter of 5′, located in the Perseus spiral arm, about 3 kpc from the Sun. There are a number of molecular clouds along the line of sight to Cas A. Three groups of features with V_{lsr} near -36, -39, and -47 km s^{-1} are located in the Perseus arm, 3 kpc from the Sun. These clouds are of special interest because the SNR Cas A provides an intense continuum background source; in the centimeter wavelength range, the surface brightness of Cas A is of order a few thousand degrees, so Cas A provides an ideal source for producing high-resolution maps using aperture synthesis techniques. Maps of H I, with angular resolution of 50″ (Schwartz et al. 1986), show smooth absorption over the entire source. Maps of OH absorption, with a resolution of 8″ (Bieging & Crutcher 1986), and H_2CO, with a resolution of 10″ (Goss, Kalberla, & Dickel 1984), show that these molecules are concentrated toward the southern part of the source and have a much more clumpy structure. For H I and OH, there have been a series of determinations of the magnetic fields from measurements of the Zeeman splitting; according to Heiles & Stevens (1986), the strength of the line-of-sight magnetic field from OH data is 9 μG; Schwartz et al. (1986) find a magnetic field strength of 50 μG from H I results.

Larger scale, lower angular resolution maps of ^{13}CO and CO emission in the regions around Cas A (see Fig. 3 of Troland, Crutcher, & Heiles 1985) show that these regions are the outer edges of larger molecular clouds. It is generally believed that these clouds are not directly interacting with the Cas A SNR, but instead are found along the line of sight. These observations have allowed a detailed investigation of the physical conditions in these regions.

The clouds at -39 and -47 km s^{-1} show absorption in the metastable $(J = K)$ lines of NH_3 (Batrla, Walmsley, & Wilson 1984). From the ratio of the populations of the (2,2) and (1,1) levels, the rotational temperatures, T_r, are 18 K, giving kinetic temperatures, T_k, of 22 K (Batrla et al. 1984). At 1.3 cm, the maximum brightness temperature of Cas A is of order 30 K, somewhat more than the kinetic temperatures of the foreground molecular clouds. The deepest NH_3 absorption is found toward the southwestern part of Cas A at -39 km s^{-1} (Batrla et al. 1984). There is also a much weaker absorption at -47 km s^{-1}, which becomes stronger toward the southeast. Because of the weakness of the line, Batrla et al. (1984) did not map the NH_3 absorption region, and the scale sizes of NH_3 in the Cas A molecular clouds were not determined. To make a size estimate for one cloud, the region of strongest NH_3 absorption was mapped with the Very Large Array.[3]

2. OBSERVATIONS

2.1. *VLA*

The observations occurred 1992 July 21 in the spectral line mode of the VLA. All available antennas were used in the VLA-D array which provides baseline lengths from 0.035 to 1.03 km. The observations of Cas A were centered at R.A. = $23^h20^m57^s.0$, Decl. = +58°32′19″.7. This pointing position is identical to Position 4 of Batrla et al. (1984). This position was chosen because it is the location of the deepest NH_3 absorption found with the 40″ beam of the 100 m. The source 3C 48 (assumed $S = 1.08$ Jy) was used as a primary flux density cali-

[1] Remote Sensing Division, Code 7200, Naval Research Laboratory, Washington, DC 20375-5351.
[2] Max-Planck-Institut für Radioastronomie, Auf Dem Hügel 69, D-53121 Bonn, Germany.

[3] The Very Large Array is an instrument of the National Radio Astronomy Observatory which is operated by Associated Universities, Inc., under cooperative agreement with the National Science Foundation.

© American Astronomical Society • Provided by the NASA Astrophysics Data System

1994ApJ...425..127G

brator. The derived flux density of the phase calibrator, 2229+695, was 0.44 Jy. The strong source 3C 84 (derived $S = 24.6$ Jy), observed twice during the session, was used for bandpass calibration. The typical observing sequence was a 4 minute scan on the phase calibrator followed by a 12 minute scan of Cas A. This sequence was repeated throughout the duration of the session. Approximately 4.8 hour of the 8 hour session was spent observing the program source, Cas A. The balance of the time was spent in calibration and in moving the telescopes.

The VLA spectral line system was used in a single IF mode. The total bandwidth of the IF was 6.25 MHz. The IF was separated into 64 channels. The first channel was a wide-band channel with a width of 4.7 MHz. The remaining 63 hanning weighted narrow channels were each 97.7 kHz wide (1.24 km s^{-1}). On-line autocorrelation normalization was used to improve the amplitude portion of the bandpass. Channel 32 of the 63 narrow channels was tuned to the rest frequency of the (J, K) = (1, 1) inversion transition of the NH_3 molecule (23.694496 GHz) at an LSR velocity of -42 km s^{-1}.

The AIPS software package of the NRAO, as implemented on NRL computer systems, was used to calibrate, reduce, and analyze the data. Antenna gain solutions were improved through the application of a self-calibration algorithm operating on the wide-band channel. The improved antenna gains were applied to the entire spectral line data set. Using an algorithm developed by Cornwell, Uson, & Haddad (1992) the u, v data in 10 line channels (4–8 and 54–58), assumed to be free of line emission, were fitted with a linear baseline, and subtracted, in the u, v plane, from the entire spectral line cube to produce a line-only data set. The data for all channels were edited and transformed into 256 × 256 pixel images (pixel size 0.″7). To maximize sensitivity, natural weighting of the data in the u, v plane was used in the Fourier transform algorithm. The FWHM beamsize of the resulting images was 3.″8 × 3.″5, p.a. −2.°6.

2.2. *IRAM*

Spectra of the $J = 1$–0 and $J = 2$–1 lines of CO and ^{13}CO were taken with the IRAM 30 m telescope in 1991 April. At the line frequencies of the $J = 1$–0 transition, the FWHP of the telescope is 21″; for the $J = 2$–1 transitions, the FWHP beamsize is 12″. A fuller account of the ^{13}CO line mapping will be given elsewhere (Wilson et al. 1993), but there is a 60″ (FWHP) cloud found in ^{13}CO centered within 30″ of the NH_3 absorption peak (cloud B of Wilson et al. 1993). We used the IRAM 30 m telescope on 1993 May 11 to obtain a ^{13}CO spectra toward the NH_3 absorption peak. The observational parameters were similar to those of the 1991 April observations. The resulting spectrum was smoothed to a velocity resolution of 0.16 km s^{-1}, and the total integration time was 30 minutes.

3. RESULTS

3.1. *VLA Continuum*

A contour plot of the 1.3 cm continuum emission from Cas A is shown in Figure 1. This plot was made from the wide-band (4.7 MHz) channel. Because the FWHM primary beam response of the VLA antennas at 1.3 cm is only 2′, we have imaged only the extreme western edge of the Cas A SNR. However, there is good agreement between this map and the 6 cm map of Braun, Gull, & Perley (1987). The image contoured in Figure 1 has been corrected for primary beam attentuation. From the peak flux density per beam, the maximum brightness temperature of the continuum emission as measured with the VLA is 33 K. From inspection of artifacts in the image plane and from u, v plots of amplitude versus projected baseline spacing it is clear that our VLA observations have missed a significant amount of the continuum emission from Cas A. This is a common problem for interferometers, which do not always adequately sample the lowest spatial frequencies. Our observations in the VLA-D array should not be sensitive to emission regions with scale sizes greater than about 1′. An estimate of the missing continuum flux density is obtained by comparing our data to the 1.3 cm, 40″ spatial resolution, single-dish data of Batrla et al. (1984). A spatial integration over our continuum map, centered on Position 4 of Batrla et al. (1984), demonstrates that the VLA data are sensitive to only about 20%–30% of the emission detected with the Effelsberg 100 m telescope.

3.2. *VLA Ammonia*

The NH_3 absorption line was only barely detected in a single synthesized beam. In order to obtain the line profile with the best signal-to-noise ratio, we summed the absorption over larger regions. The spatial integrations were performed in regions of the spectral line image cube where appreciable continuum emission was found in the continuum channel. The strongest NH_3 absorption was found against the peak continuum emission near R.A. = $23^h20^m54^s.8$, Decl. = +58°32′23″; however, NH_3 absorption was found over the entire continuum structure bracketed in Figure 1. This indicates that the NH_3 cloud responsible for the absorption has a minimum size of 60″. A spectrum of the NH_3 absorption is shown in Figure 2a. This spectrum was obtained by integrating the line emission over the region indicated in Figure 1, but only in locations

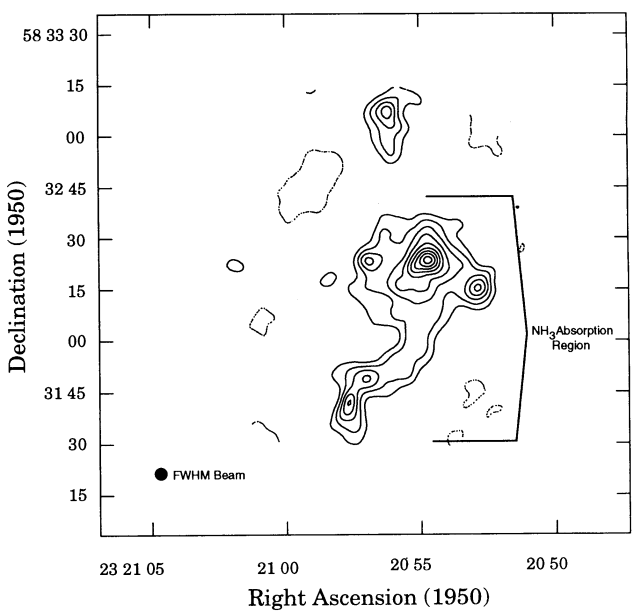

FIG. 1.—A 3.″8 by 3.″5 resolution VLA map of the 1.3 cm continuum emission from Cas A. The contours are −15, 15, 25, 35, ... 95% of the peak flux density (186 mJy $beam^{-1}$). Because the FWHM primary beam response of the VLA antennas at 1.3 cm is only 2′, we have imaged only the extreme western edge of the Cas A SNR. A primary beam correction has been applied to this image. NH_3 absorption is found over the bracketed region. The FWHM beam is indicated in the lower left.

© American Astronomical Society • Provided by the NASA Astrophysics Data System

1994ApJ...425..127G

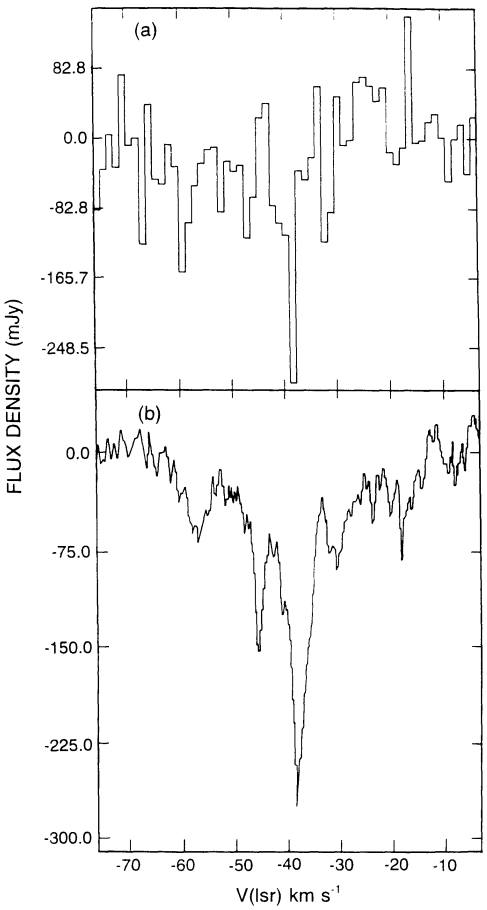

FIG. 2.—(*a*) A VLA spectrum of (J, K) = (1,1) NH_3 obtained by integrating the line emission over the region indicated in Fig. 1, but only in locations where the continuum flux density was above 37 mJy beam^{-1} (20% of the peak flux density in the map). The velocity resolution is 1.2 km s^{-1}. (*b*) The single-dish 100 m NH_3 (1,1) profile toward Position 4 of Batrla et al. (1984) with a FWHP beam of 40″.

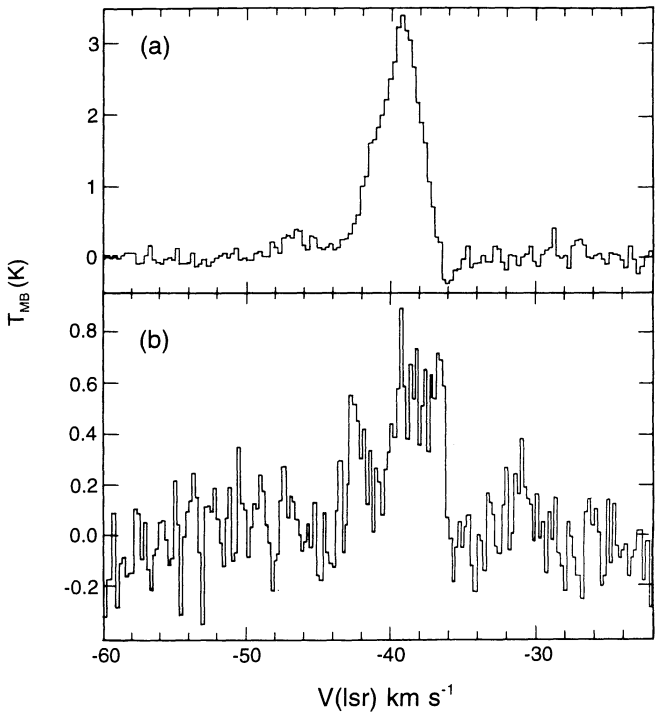

FIG. 3.—(*a*) IRAM spectrum of the J = 1–0 line of ^{13}CO with a velocity resolution of 0.3 km s^{-1}. This spectrum was taken at the emission peak of cloud B of Wilson et al. (1993) with a FWHP beam of 21″. (*b*) IRAM spectrum of the J = 2–1 line of ^{13}CO with a velocity resolution of 0.2 km s^{-1}. This spectrum was taken at the position of maximum NH_3 absorption. The FWHP beam is 12″.

where the continuum flux density was above 37 mJy beam^{-1} (20% of the peak flux density in the map, 6 times the rms noise level).

Single-dish NH_3 (J, K) = (1, 1) and (2, 2) absorption measurements have been made with the 100 m telescope and are presented by Batrla et al. (1984). Figure 2*b* shows their (J, K) = (1,1) absorption profile at Position 4. A spatial integration over the VLA line cube, centered on Position 4 of Batrla et al. (1984), demonstrates that our VLA data are sensitive to only 60% of the line absorption detected with the 100 m telescope. This indicates that the NH_3 cloud has some spatial structures larger than about 60″. The total optical depth (see Batrla et al. 1984) in the NH_3 absorption line is $\approx$0.1. This is significantly larger than the total optical depth, 0.027, derived from the 100 m observations at Position 4 of Batrla et al. (1984). The difference can be attributed to the different line-to-continuum ratio derived from our VLA data. The VLA data detects only 23% of the 100 m continuum emission at Position 4 but detects 64% of the line absorption.

3.3. *Kinetic Temperatures*

Spectra of the ^{13}CO emission toward the Cas A NH_3 cloud are shown in Figure 3. Figure 3*a* is the J = 1–0 line toward the emission peak of Cloud B of Wilson et al. (1993). Figure 3*b* is the J = 2–1 line toward the NH_3 peak. In the following, we compare the CO and ^{13}CO emission and NH_3 absorption line results, using the assumption that these species arise from the same region. This assumption is supported by the similar spatial distributions, radial velocities, and line widths of these species.

Our VLA data shows that the NH_3 emission is extended compared to the 40″ beam of the 100 m. Therefore, the value of T_k obtained from the 100 m data, 22 K, is relevant for this region (Batrla et al. 1984). Maps show that the CO line emission regions are extended compared to a 20″ beam, and the filling factor is unity. As is usual, we assume that the CO J = 1–0 line emission is optically thick and thermalized, so the peak brightness temperature equals the local kinetic temperature, T_k. From our CO data, the local value of T_k is 18 K. Thus, the values of T_k obtained from CO and NH_3 measurements are nearly equal.

3.4. *Column Density of CO*

In Table 1 we present various physical parameters derived from the CO data. A more detailed discussion of the derivation of these parameters is given in Wilson et al. (1993). By applying the Large Velocity Gradient (LVG) approximation (see, e.g., Goldsmith, Young, & Langer 1983) to the (assumed optically thin) J = 2–1 and J = 1–0 lines of ^{13}CO, the local H_2 number density can be determined. The peak column density of H_2 has been obtained from our LVG analysis also. It is likely that the outer part of this H_2 cloud is surrounded by a layer of H I. Frerking et al. (1982) find that an H I column density of 10^{21}

© American Astronomical Society • Provided by the NASA Astrophysics Data System

1994ApJ...425..127G

TABLE 1

DERIVED PARAMETERS FROM CO AND ^{13}CO DATA[a]

Parameter	Value	Mass from ^{13}CO ($M_\odot$)	Virial Mass ($M_\odot$)
^{13}CO line ratio[b,c]	0.61 (0.04)	16	10^3
$\Delta V_{1/2}$[c] (km s^{-1})	3.5 (0.2)		
V_{lsr}[c] (km s^{-1})	−39.3 (0.1)		
$n(H_2)$ (cm^{-3})	10^3		
$N(H_2)$ (cm^{-2})	3×10^{21}		

[a] For cloud of FWHP size 60″, centered at R.A. = 23^{h}20^{m}52^s.4, Decl. = +58°32′18″ (1950.0).
[b] Ratio of integrated $J = 2$–1 to $J = 1$–0 ^{13}CO intensities.
[c] From Gaussian fits; rms errors are given.

TABLE 2

RELATIVE ABUNDANCES OF VARIOUS MOLECULAR SPECIES[a]

Species	Abundances
X(H I)	3.6×10^{-2}[b]
$X(H_2CO)$	3×10^{-8}[c]
$X(NH_3)$	1×10^{-8}[d]
X(OH)	4×10^{-7}[e]

[a] Using $N(H_2)$ from Table 1.
[b] From Fig. 2 of Schwartz et al. 1986.
[c] From Goss et al. 1984, column density also quoted in Batrla et al. 1984.
[d] Batrla et al. 1984.
[e] Using our Table 1, together with the column density for feature I of Bieging & Crutcher 1986.

cm^{-2} is needed to shield the CO against the interstellar radiation field. This would increase the $N(H_2)$ value in Table 1. Neglecting this H I contribution, we have obtained the masses of the molecular cloud. The virial theorem estimate gives 1000 solar masses. This is 60 times the mass obtained from integrating the ^{13}CO column density over the cloud.

4. DISCUSSION

4.1. *The Kinetic Temperatures of the Clouds*

On the basis of our NH_3 absorption data and previous absorption line results, and our CO emission data, the region investigated is significantly warmer than a typical dark dust cloud, and shows a line width which is significantly larger than found for dark clouds. However, the region has local number and column densities that are comparable to dark dust cloud values.

It is generally accepted that values of $T_k = 10$ K are caused by cosmic-ray heating (see, e.g., Hollenbach 1988). Since this cloud is warmer, an additional heating mechanism is required for the cloud observed here. The equality of the values of T_k obtained from NH_3 and CO will constrain any heating mechanism. Heating caused by massive stars embedded in the cloud could provide the T_k found from the CO data (see, e.g., Hollenbach 1988). CO is a sturdy molecule (dissociated by 11 eV photons), but NH_3 is comparatively fragile (dissociated by 4 eV photons) and would be destroyed rather than heated if massive stars were nearby. The argument against heating by the interstellar radiation field is similar. However, in discussing observations of cirrus molecular clouds, Turner (1993) has favored such a mechanism, noting that an enhanced NH_3 formation rate (by some unknown process) is needed. The luminosity of the entire cloud containing the NH_3 is 40 solar luminosities. To provide this, only a few A-type stars are needed (see, e.g., Allen 1963). Admittedly, although these stars will heat dust grains, heating of the gas molecules will be less effective, since the low H_2 density prevents an effective coupling of gas and dust temperatures.

The line-of-sight magnetic field strength from these molecular clouds has been measured to be 9 μG (see, e.g., Heiles & Stevens 1986). If the total magnetic field strength is ≈ 15 μG, this strength is so low that ion slip heating would not be very effective. Myers & Goodman (1968) assumed the magnetic energy equals the gravitational of kinetic energy. Then the magnetic field strength is predicted to be 190 μG, and ion-slip heating would be viable.

Other promising heating mechanisms involve either an enhanced cosmic-ray rate (by a factor of 1.5 above the local value) or cloud-cloud collisions. The higher cosmic-ray rate would also increase the H I fractional abundance. As shown in Table 2, there is a fairly large amount of H I in this direction. If associated with the NH_3 cloud, the enhanced H I abundance indicates that cosmic-ray heating might be significant. The CO and NH_3 line widths are enhanced with respect to values found for dark dust clouds. This might suggest heating via cloud-cloud collisions. Such a heating mechanism could heat the interiors of clouds effectively. This might help to explain the comparable values of T_k obtained from NH_3 and CO. If the 3.5 km s^{-1} line width were caused by a single shock, the NH_3 would be dissociated. Thus, it is likely that this is a C-type shock, or a collection of slower shocks.

4.2. *The Relative Abundance of Molecular Species*

In Table 2 we have collected the abundances of different molecular species relative to H_2 from measurements toward the NH_3 maximum. It is clear that the relative abundance of OH is within a factor of 2 of that estimated for dark dust clouds such as TMC1 (see, e.g., Table VIII of Irvine et al. 1985). The H_2CO abundance in the cloud is larger than in TMC1 by a factor of 3. Given the uncertainties, these abundances are in reasonable agreement with the abundances obtained for TMC1. On the other hand, there seems to be a definite deficit of polyenes in this cloud, relative to TMC1, based on unpublished limits to the optical depth of the $J = 1$–0 line of HC_3N.

5. CONCLUSIONS

A measurement of the $(J, K) = (1, 1)$ inversion line of NH_3 in absorption toward Cas A with the VLA using a 3.″8 × 3.″5 synthesized beam, and CO and ^{13}CO line measurements with the IRAM 30 m telescope allow us to draw the following conclusions:

1. Comparisons of the optical depths and line flux densities of the NH_3 absorption region show that the region displays structure on size scales from 10″ to more than 60″.
2. The kinetic temperature obtained from NH_3 absorption and CO emission agree well; the value is somewhat more than 20 K. The heating mechanism is uncertain; three possibilities are ion-slip heating if the magnetic field is large, an enhanced cosmic-ray rate, perhaps arising from the SNR, or heating from shocks, related to cloud-cloud collisions.

© American Astronomical Society • Provided by the NASA Astrophysics Data System

1994ApJ...425..127G

3. If kinetic energy is balanced only by gravitation, the virial cloud mass is 60 times the value obtained from CO data. Thus, this region is not stable.

4. The H_2 column density for the nearest molecular clump allows us to determine the relative abundance of NH_3, H_2CO, OH, and H I. These values are similar to the dark dust cloud TMC1, except there is a larger abundance of H I and a much lower abundance of polyenes. Alternatively, if the larger line widths are cause by magnetic broadening, the inferred field strength must be greater than 9 μG, the measured line-of-sight value.

T. L. W. and K. J. J. were supported in part by the Max-Planck-Forschungspreis, administered by the A. von Humbold-Stiftung. The authors wish to thank P. F. Bowers and A. L. Fey for a careful reading of this manuscript. Basic research in radio interferometry at the Naval Research Laboratory is supported by the Office of Naval Research.

REFERENCES

Allen, C. W. 1963 Astrophysical Quantities (London: Athlone), 203
Batrla, W., Walmsley, C. M., & Wilson, T. L. 1984, A&A, 136, 127
Bieging, J. H., & Crutcher, R. M. 1986, ApJ, 310, 853
Braun, R., Gull, S. F., & Perley, S. R. 1987, Nature, 327, 395
Cornwell, T. J., Uson, J. M., & Haddad, N. 1992, A&A, 256, 583
Frerking, M. A., Langer, W. D., & Wilson, R. W. 1982, ApJ, 262, 590
Goldsmith, P. F., Young, J. S., & Langer, W. D. 1983, ApJS, 51, 203
Goss, W. M., Kalberla, P. M. W., & Dickel, H. R. 1984, A&A, 139, 317
Heiles, C., & Stevens, M. 1986, ApJ, 301, 331
Hollenbach, D. 1988, Ap. Lett. Comm., 26, 191
Irvine, W. M., Schloerb, F. P., Hjalmarson, A., & Herbst, E. 1985, in Protostars and Planets II, ed. D. C. Black & M. S. Matthews (Tucson: Univ. Arizona Press), 579
Myers, P., & Goodman, A. 1988, ApJ, 326, L27
Schwartz, U. J., Troland, T. H., Albinson, J. S., Bregman, J. D., Goss, W. M., & Heiles, C. 1986, ApJ, 301, 320
Troland, T. H., Crutcher, R. M., & Heiles, C. 1985, ApJ, 298, 808
Turner, B. 1993, ApJ, submitted
Wilson, T. L., Mauersberger, R. M., Muders, D., Przewodnik, A., & Olano, C. 1993, A&A, in press

© American Astronomical Society • Provided by the NASA Astrophysics Data System